Time-resolved flow measurements with fast-response aerodynamic probes in turbomachines

To cite this article: Peter Kupferschmied *et al* 2000 *Meas. Sci. Technol.* **11** 1036

View the article online for updates and enhancements.

Related content

- Time-resolved entropy measurements using a fast response entropy probe

- A fast response miniature probe for wet steam flow field measurements

- A flow field investigation in the diffuser of a high-speed centrifugalcompressor using digital particle imaging velocimetry

Recent citations

- Plasma pressure sensor based on direct current glow discharge
  Fan Li *et al*

- Design and Testing of a Miniaturized Five-Hole Fast Response Pressure Probe With Large Frequency Bandwidth and High Angular Sensitivity
  Elissavet Boufidi *et al*

- Characterization of the Unsteady Aerodynamics of Optimized Turbine Blade Tips through Modal Decomposition Analysis
  Bogdan C. Cernat and Sergio Lavagnoli

Time-resolved flow measurements with fast-response aerodynamic probes in turbomachines

Peter Kupferschmied, Pascal Köppel, William Gizzi, Christian Roduner and Georg Gyarmathy

ETH Zurich (Swiss Federal Institute of Technology), Institute of Energy Technology, Turbomachinery Laboratory, CH-8092 Zurich, Switzerland†

Abstract. A better understanding of unsteady flow phenomena encountered in rotor–stator interactions is a key to further improvements in turbomachinery. Besides CFD methods yielding 3D flow field predictions, time-resolving measurement techniques are necessary to determine the instantaneous flow quantities of interest. Fast-response aerodynamic probes are a promising alternative to other time-resolving measurement techniques such as hot-wire anemometry or laser anemometry.

This contribution gives an overview of the fast-response probe measurement technique, with the emphasis on the total system and its components, the development methods, the operation of such systems and the data processing requirements. A thorough optimization of all system components (such as sensor selection and packaging, probe tip construction, probe aerodynamics and data analysis) is the key of successful development.

After description of the technique, examples of applications are given to illustrate its potential. Some remarks will refer to recent experiences gained by the development and application of the ETH FRAP® system.

1. Introduction

Turbomachinery flows are highly unsteady due to the relative motion of rotating and fixed blade rows. In general the frequency spectrum of the fluctuations covers a broad range extending to several multiples of the blade passing frequency. Typically a range of 0 to 50 kHz may be of practical interest in aerodynamic (gaseous-flow) turbomachines.

The fluctuations may be separated into periodic and stochastic ones. Predominantly, periodic fluctuations arise from the regular passing of wakes and other non-uniformities (such as secondary and leakage flow patterns or shocks etc) over the blades and their frequency is a multiple of the rotor revolution frequency. Nearly periodic unsteadiness may arise from large-domain unsteady phenomena such as rotating stall or mild surge in compressors. Stochastic fluctuations can be due to turbulence, to unsteady transition and separation of boundary layers or to intermittent blade flutter. All these unsteady effects have to be detected by measurement systems to understand the loss mechanism and unsteady running conditions. An excellent overview of measurement techniques for unsteady flows in turbomachines is given in Sieverding *et al* (2000).

† http://www.lsm.ethz.ch

It is desirable that fast-response measurements identify and document all types of fluctuation. This contribution discusses the requirements to be made towards fast-response aerodynamic probe systems used for exploring turbomachinery flows, the types and the performance of probes and examples of their application.

Probes developed for turbomachinery usually have one, two or more pressure sensors accommodated in the probe tip. The sensor pressures do not, in general, correspond to the total or static pressure of the undisturbed flow, but may be converted into these (and into flow angles and velocity) by calibrating the probe under well controlled flow conditions. Probes with several sensors are theoretically capable of measuring total pressure, static pressure, flow velocity (and Mach number) and flow direction (yaw and pitch angles with respect to the probe head). The time resolution often exceeds 50 kHz bandwidth. In order to make reliable measurements, high precision calibration in special calibration facilities, comprehensive mathematical modelling and automated statistical treatment of massive amount of redundant data are required. (The latter task is specific to time resolving measurements. The classic pneumatic probe directly measures averaged data, due to its inherently high time lag.) Sensor-based probes may in principle be used for measuring flow temperature thanks

to the temperature sensitivity of sensor chips. The time resolution is typically low (<1 Hz) and special calibration is needed.

In most applications the objective is to achieve the same accuracy in both the AC and the DC part of the highly fluctuating flow quantities. This poses high demands on the probe technology (design, construction, materials) as well as calibration and measurement procedures. Large parts of the present paper are devoted to these problems. In the nearly three decades of fast-response probe development the efforts were focused on the AC component. Significant improvements achieved a DC accuracy comparable to that of pneumatic probes.

Aerodynamic probes are usually mounted on the casing (stator) part and immersed into the unbladed space separating the stator and rotor rows. Probe traverses within blade channels are problematic due to blockage effects caused by the finite dimensions of the probe. Here non-intrusive (optical) methods are more attractive. While rotor mounted pneumatic probes have been variously reported in the literature, fast-response probes seem to have been restricted, at least up to the present, to the non-rotating parts where their practical application is straightforward and requires little modification of the machine to be investigated.

2. The fast-response probe technique

2.1. Overview

After the simple bent tube used first by Henri Pitot in 1732 to measure the total pressure in fluid flow, a broad variety of pneumatic pressure probes has been developed over the years (see e.g. Bryer and Pankhurst 1971, Chue 1975). Depending on the velocity range and angular range required, different turbomachinery-specific probe head geometries have been designed. All these probes can determine one or more flow quantities such as total and static pressure, flow angles or Mach number by measuring the pressures at different locations on the probe tip. However, the signal damping resulting from the pneumatic lines between the tip bores and the pressure transducers confined this technique to time averaged flow information only. Of course, this is a severe limitation regarding the unsteady and complex nature of turbomachinery flows, which rather demands a continuous measurement at several points in space with a bandwidth sufficient to determine the physical flow quantities of interest.

In the early 1970s, the progress in the size of pressure sensors made possible the building of probes with the sensor(s) installed closer to the probe taps, thus strongly improving their dynamic characteristics. Larguier and Ruyer (1972) mounted a single piezoelectric sensor into the probe tip and used it for time-resolved measurements in air flows. The attributes of this design were the increased flow disturbances due to a rather large probe tip diameter of 8 mm. To reduce the tip size, Senoo *et al* (1973) and Matsunaga *et al* (1978; figure 1) used probes with several sensors in the probe shaft. Due to this sensor configuration, the bandwidth decreased to 1 kHz and confined the application to measurements in water flows.

Probes hosting several sensors directly on the tip surface or in the tip interior could be realized by using small
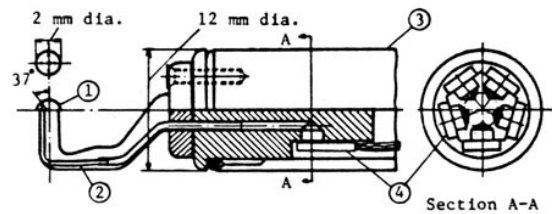

Figure 1. Five-hole probe with 2 mm diameter probe tip designed for application in water flows. The pressure sensors are located in the 12 mm diameter shaft part (Matsunaga *et al* 1978).
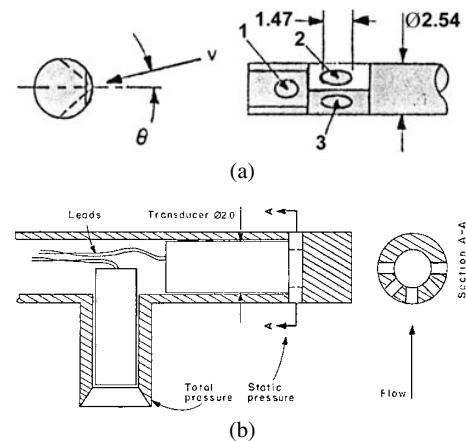

(a)

(b)

Figure 2. Early fast-response probes developed for the MIT Blowdown Compressor Facility (Kerrebrock *et al* 1974). The cylinder probe (a) used for flow field surveys downstream of the rotor was equipped with three surface-mounted silicon pressure diaphragms. The flow field upstream was measured with a total-static fast-response probe (b) containing two standard commercial sensors.
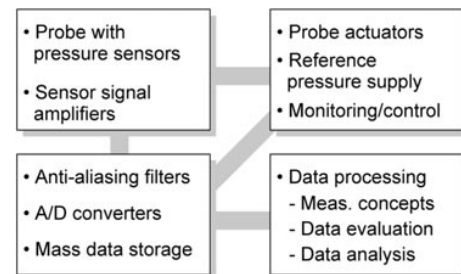

Figure 3. Schematic of the main components of a fast-response pressure probe measurement system.

piezoresistive silicon pressure sensors made available in the seventies (figure 2). Analogue bandwidths of 30 kHz and even more could thus be achieved. From then on, several research groups around the world have developed their own probes tailored to their applications. Some of these designs will be presented in section 3.2. The main system components necessary to operate fast-response probes are similar for all systems (figure 3).

Not only the sensor and probe technology took benefit from the great advances in microtechnology, microelectronics and computer sciences, but also the required high-speed data acquisition technique and the data processing technology. The high analogue bandwidth (typically 50 to 100 kHz) necessary for time-resolved turbomachinery flow

Table 1. Comparison of different flow measurement techniques (Kupferschmied 1998).

Comparison criteria	Hot-wire anemometer	Laser Doppler anemometer	Fast-response aerodynamic probes
Measured quantities			
Time series	available	not available	available
p_{tot} and p_{stat}	not available	not available	good (DC and AC)
Temperature	special care required	not available	DC: good, AC: poor
Flow velocity vector	DC: difficult, AC: very good	DC: very good, AC: good	like Mach number, DC temperature measured with probe
Mach number	high speed: limited temperature has to be known (then like velocity)	high speed: difficult (data rate) temperature has to be known (then like velocity)	low speed: limited good (DC and AC)
Measurement position			
Max. temperature and pressure	high temperature and pressure: difficult	suited for high temperature and pressure	T_{max}: 140 (200) °C p_{max}: several bar
Access requirements for measurement position	low (bore and probe actuator)	high (optical window)	low (bore and probe actuator)
Requirements to flow	high (good filters)	high (seeding)	low
Flow disturbance (probe head)	low–medium	nonexistent–low	medium (modern probe)
Measurements in rotor	difficult	good	difficult
Long time measurements (e.g. monitoring)	not suited	possible	good
Operating aspects			
Calibration effort	high	low (seeding contr.)	medium–high
Calibration validity	short	very long	long
Equipment complexity	medium	high	medium
Operating flexibility	medium	low–medium	high
Life-time of probe tip	short	very high	high
Data amount/measuring time	high	low–medium	high
Data processing	complex	complex	complex
Estimated system price	70 000 USD	250 000 USD	100 000 USD

measurements and the massive number of data produced require electronic hardware that was too expensive for widespread use in the past.

2.2. Requirements toward time-resolved flow measurements

Relevant flow quantities are defined from thermodynamics and aerodynamics and determine the essential characteristics of a measurement system:

(i) total and static pressure and temperature;
(ii) flow angle and velocity and
(iii) turbulence structure and distribution functions.

Depending on the specific measurement task to be accomplished an aerodynamic probe measurement system has to fulfil several features. The features to be considered—which can be crucial for the desired measurement quality—are the following:

(i) *Frequency bandwidth.* For the determination of systematic pressure fluctuations, small turbulence length scales or the wake momentum thickness, high harmonics of the blade passing frequency should be resolved. This requires a frequency response of the probe and the data acquisition system capable of resolving typical blade passing frequencies of 5–10 kHz and their first three to five harmonics.
(ii) *Spatial resolution.* The probe tip has to be smaller than the significant flow structures to be resolved. Therefore

a strict reduction of the probe tip size, which often has to incorporate several sensors, is of utmost importance. In this way aerodynamic measurement errors caused by the presence of the probe tip in the flow can be kept under control, see section 3.
(iii) *Accuracy.* The accuracy of the measurement instrument—the probe—is influenced from two different directions: pressure measurement errors caused by the use of miniature piezoresistive sensors and aerodynamic errors caused by the finite probe tip size and the chosen external geometry, see section 3.
(iv) *Resolution and signal to noise ratio (SNR).* For turbulence measurements under marginal flow conditions (e.g. low Mach number or low density) the level of resolution and of signal to ratio pose challenging demands to the data acquisition system and the aerodynamic probe with its sensors (e.g. a resolution of a few Pascal).
(v) *Pressure and temperature level.* In typical turbomachinery flows the pressure level can range from vacuum (blow down facilities) to several bar. Often this may be connected with high gas flow temperatures. Then the sensors have to be capable of measuring the pressure fluctuations without being affected by thermal noise or material damage.

2.2.1. Comparison with other techniques. Table 1 compares the characteristics of the fast-response aerodynamic probe technique, of hot wires and of LDV. Each measurement technique has its advantages and drawbacks, and can
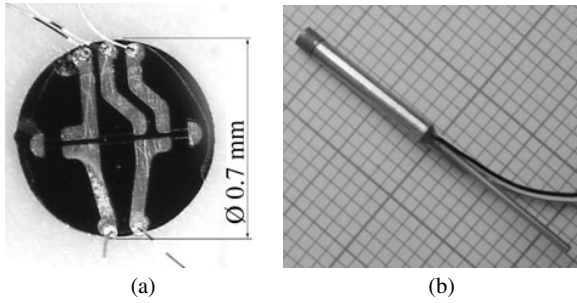
Figure 4. (a) Silicon membrane with pressure sensitive middle part. (b) Standard commercial sensors with electric connections and reference pressure port tube (differential pressure mode).

Figure 5. (a) Piezoresistive miniature pressure sensor chip (die), typical size $1.7 \times 0.6 \times 0.2$ mm^3. (b) Schematic of the typical Wheatstone bridge deposited on the diaphragm.

Figure 6. Typical output signal U and excitation signal U_e of a miniature piezoresistive pressure sensor chip as a function of temperature and pressure (Sensym P788, excitation current 1 mA).

be considered as complementary to the others. Prominent advantages of the aerodynamic probe technique are its ability to measure pressure within the flow (total and static, AC and DC), its robustness in comparison to hot-wire probes and its simplicity in practical use in comparison to optical techniques. A wide variety of unsteady flows measurement techniques for turbomachinery has been reviewed by Sieverding *et al* (2000).

3. Fast-response probes

3.1. Miniature pressure sensors

As discussed later, the size of the probe should be as small as possible to reduce both time-independent and time-dependent measurement errors. Since the geometry and the size of the probe depends strongly on the pressure sensor design, the availability of appropriate sensors is crucial.

Although piezoelectric pressure sensors have also been used in early years, the requirements in terms of size, pressure sensitivity and the objective of accurately measuring also the DC part of the pressure signal reduce the choice to piezoresistive or capacitive pressure sensors. Preference is given to the piezoresistive principle (Binder 1989) which does not require any signal conditioning on the sensor itself. They also have the best pressure sensitivity when miniature size is required.

Most probe designs listed in table 2 accommodate standard commercial piezoresistive pressure sensors produced by companies like Kulite, Endevco or Entran. While some of these sensors have been used as bare silicon membranes (figure 4(a)) in earlier developments (e.g. Kerrebrock *et al* 1974), they are mostly used as completed units, i.e. the semiconductor sensor chip is mounted in its own casing (figure 4(b)). However, these types are either too large to fit into really miniature probes or they have generally an insufficient pressure sensitivity.

A good alternative to avoid the size increase due to such a double containment is provided by raw pressure sensor chips (dies, figure 5) used e.g. in biomedical applications. Of course, the chip encapsulation into the probe tip is more challenging, since the packaging and all electric and pneumatic connections have to be achieved in a sub-millimetre space.
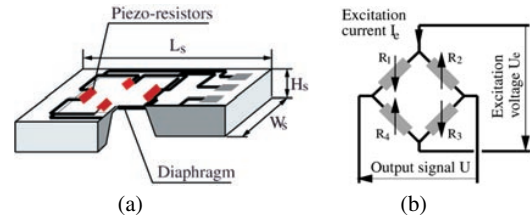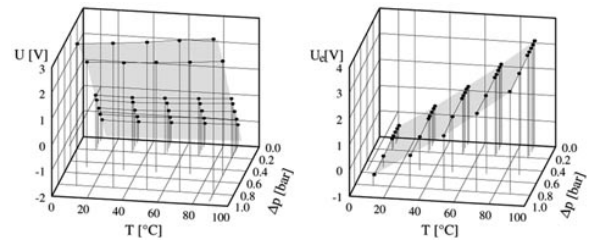
3.1.1. Sensor properties. Assuming a constant excitation current I_e in the Wheatstone bridge circuit diffused onto the thin diaphragm (figure 5(b)), the output signal voltage depends strongly on the pressure applied on the diaphragm, and weakly on temperature. On the other hand, the excitation voltage U_e is weakly dependent on the pressure, but strongly on temperature (figure 6). This enables the pressure sensor to measure also the diaphragm temperature.

The temperature changes also affect the pressure sensitivity and the pressure zero signal and must be compensated to achieve a good accuracy. Whereas passive compensation methods with external resistor circuits are still widely used (reviewed in Epstein 1985 and Sieverding *et al* 2000), active methods using the temperature information gained from the total Wheatstone bridge resistance are now well established. They operate either with active analogue circuits (Cherrett 1990) or with numerical models based on extensive calibration data (Gossweiler *et al* 1990, 1995) and offer a higher accuracy over a wide temperature range. The numerical approach accounts also for the non-linearities.

3.1.2. Selection criteria. The following basic criteria may be applied in selecting sensor chip types and individual sensors for pressure probes (Kupferschmied *et al* 1999):

(i) *Pressure range.* In contrast to absolute-pressure sensors, whose reference side of the membrane (cavity) is evacuated, differential sensors can operate in much larger pressure ranges: the common pressure level (in the turbomachine) acting on the flow-side of the diaphragms can be rudimentarily compensated by supplying an appropriate reference pressure to the probe interior. This mode not only enhances the pressure sensitivity of the sensors, but also allows us to readjust the sensor's gain and zero during the application. This is of great advantage for an accurate measurement of the DC signal

Table 2. Some characteristics of major fast-response probe designs. The wedge probes listed have a 30° apex angle. The size refers to the probe diameter or the side length [mm]. A: absolute, D: differential pressure sensor; G: gaseous flows, W: water flows.

Author		Probe tip	Size	Sensors	Fluid
Larguier and Ruyer	1972	cylinder	∅ 8	1 (piezoelectric)	G
Senoo *et al*	1973	cobra		5, in shaft	W
Kerrebrock *et al*	1974	cylinder	∅ 2.6	3, on surface	G
Castorph	1975	cone	∅ 8	6	W
Matsunaga *et al*	1978	hemisphere	∅ 2.0	5 A, in shaft	W
Shreeve *et al*	1978	Pitot	∅ 2.1	1 D	G
Kerrebrock *et al*	1980	sphere	∅ 5.1	5 A, diaphragm	G
Heneka	1983	wedge	5.5	4 D (7bar)	G
Larguier	1985	pyramid	∅ 7.0	5	G
Epstein	1985	cylinder	∅ 3.3	4, on surface	G
Ng and Poppernack	1987	pyramid	∅ 5.2	4 D	G
Bubeck and Wachter	1987	wedge	6.0	3 A, DC w. pneumatic lines	G
Cook	1989	wedge	5.6	3 A (3.4 bar)	A
Gossweiler *et al*	1990	cylinder	∅ 2.5	4 D, inside	G
Ainsworth *et al*	1995	pyramid	n/a	3	G
Kupferschmied *et al*	1994	Pitot	∅ 0.8	1 D, inside	G
		cylinder	∅ 1.8	3 D, inside	G
Brouckaert *et al*	1998	cylinder/ellipse	∅ 3.0	3 A, inside	G

part, considering the limited stability of microsensors due to hysteresis and drift effects.

(ii) Although some sensitive sensor chips are designed for pressure differences up to 350 mbar only (biomedical types), they in fact can be used up to several bar without mechanical damage. If a numerical model-based signal processing is chosen (see section 4.1), all non-linearities occurring in this case are taken into account by using extensive calibration data.

(iii) *Pressure sensitivity.* Sensors with a smaller pressure range show *per se* a better pressure sensitivity. Also, it is helpful to normalize the sensitivity with the sensor excitation power to estimate the heat dissipation of the sensor diaphragm—which strongly affects the DC stability of the pressure signal.

(iv) *Sensor geometry and size.* They should match the general shape and size of the probe (see also section 3.2). Due to the vacuum containment, absolute pressure sensor chips are generally slightly larger than differential ones.

(v) *Total resistance of the Wheatstone bridge (figure 5(b)).* Higher bridge resistance and long electric lines to the amplifiers affect the amplitude and phase response of the system and should be accounted for in high-performance applications.

(vi) *Temperature sensitivity.* A higher temperature coefficient provides a better resolution of the diaphragm temperature measurement, but is problematic for electronically compensated sensors.

(vii) *Signal stability.* A high accuracy of both AC and DC parts of the pressure signal relies on stable sensor signals. Remaining errors can be corrected to some extent by applying appropriate measurement concepts.

(viii) *Maximum temperature.* Biomedical pressure sensor chips are machined from monocrystalline silicon. The resistor noise (leakage current due to p–n junction) of the semiconductor material limits the operating temperature to 120–140 °C, depending on the doping level.

3.1.3. Development trends. Higher probe operating temperatures are a clear objective for applications such as in high-performance compressor stages. Microtechnologies for miniature chips based on silicon-on-insulator (SOI) with temperature limits of 240 °C and more exist on a prototype level (e.g. Lisec *et al* 1996). However, no commercial chips with comparable size are commercially available yet.

3.2. Development of fast-response probes

Instead of simply 'converting' conventional pneumatic probe designs into fast-response probes, the development is a longer optimization process with the following issues to achieve optimal probe characteristics:

(i) optimization of the probe shape;
(ii) miniaturization of the probe size;
(iii) mechanical optimization of the probe and
(iv) optimization of sensor packaging.

3.2.1. Aerodynamic design. Fast-response aerodynamic probes often face highly fluctuating flow conditions with large flow angle and velocity fluctuations. Therefore the aerodynamic design involves both time-independent and time-dependent aerodynamic criteria.

Size and shape are key factors. The smaller the probe, the better is its spatial resolution and faster its adaptation to changing flow conditions. The measurement errors in inhomogeneous or unsteady flow are found to be strictly proportional to probe size (Humm *et al* 1994). Therefore the probe body has to be miniaturized as far as possible under consideration of manufacturing and sensor packaging limitations. For typical probe tip dimensions reported in the literature see table 2.

Even more important is the correct choice of an appropriate probe body geometry. The main goal of shape design is to achieve a good compromise between high sensitivity to flow angle variations in steady flow
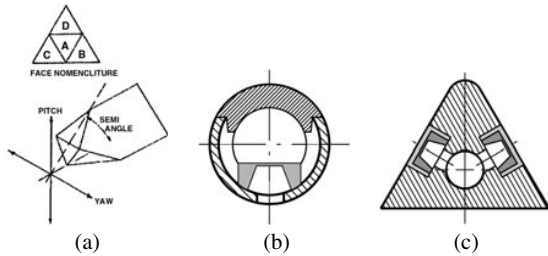
Figure 7. Fast-response probe geometries derived from pneumatic probes (Ainsworth *et al* 1995 (a), Gossweiler *et al* 1990 (b), (c)).

and small dynamic errors in unsteady flow. The latter means that the aerodynamic characteristics of the probe body do not change over the fluctuation frequency range of interest (Humm 1996). During the last decades of pneumatic probe development extensive research has been done about time-independent probe characteristics. Cylindrical probe geometries are found to exhibit good aerodynamic characteristics in term of Reynolds number ($\mathrm{Re} = 10^3$–10^5) and Mach number values (0.2–0.9).

The time-dependent aerodynamic characteristics are crucial in order to avoid uncorrectable measurement errors caused by the inertial behaviour of the local flow around the probe body during changing overall flow conditions. In the past years different pneumatic designs were used for the development of fast-response aerodynamic probes (table 2).

Recently, extensive aerodynamic research has been performed concerning aerodynamic time-dependent effects on probes (e.g. added mass, dynamic stall) with different geometries to extend the knowledge about time-dependent probe aerodynamics (Kovasznay 1980, Humm *et al* 1992, 1994, Humm 1996). It was found that each probe body shape, i.e. those shown in figure 7, induces reproducible (i.e. systematic) measurement errors in flows subjected to controlled fluctuations at a given reduced frequency k. The errors increase with k and with the amplitude of fluctuations. Cylindrical probes were found to produce the least error, as illustrated in figure 8 for the case of $k = 0.1$.

Correction procedures for the reduction of the remaining time-dependent errors are under development (Gizzi 2000). Based on these experiences the FRAP system uses straight cylindrical probes only.

3.2.2. Mechanical design.
Straight shafts without hooks are preferentially used in turbomachinery in order to facilitate access to the flow space, particularly between narrow blade rows. The shaft should withstand aerodynamic forces or vibrational excitation but remain as thin as possible.

The design of the probe tip is dictated by several considerations:

(i) *Sensor operating mode*. Whereas absolute sensors are quite useful in transient test facilities, differential sensors are more advantageous in continuous flow facilities because the pressure zero-offset and gain can be readjusted *in situ*. However, a reference pressure lead has to be provided to the interior of the probe tip.

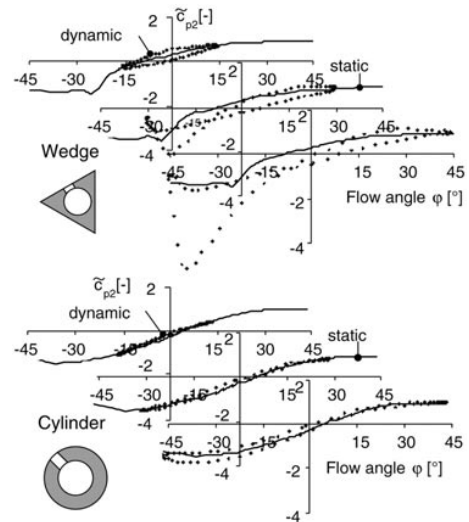(ii) *Sensor position in wedge probes*. Due to the flank geometry, the side taps of wedge probes are predestined

Figure 8. Dynamic response of the lateral-tap pressure coefficient c_{p2} of a 60° wedge and a cylinder probe due to relative flow yaw angle oscillations with a reduced frequency of $k = 0.1$ and different yaw angle amplitudes ($\hat{\varphi} = 15°; 30°; 45°$). The crosses represent the sensor response in uniform steady flow while the probe performed controlled oscillations in yaw. The solid line is the yaw dependence of c_{p2} obtained by static calibration. In the dynamic response of the wedge the deep pressure valley was identified to be caused by dynamic stall (Humm *et al* 1992).

for surface-mounted flat sensor chips (Cook 1989, Bubeck and Wachter 1987; figure 9(a)). Ainsworth *et al* (1990) developed a technique to mount them onto the metal surface of turbomachine blades and applied it also to wedge probes. Due to the exposure of the diaphragms to particles entrained in the flow, metal screens or special silicone rubber coatings are generally used as a protective cover. Heneka (1983) avoids this problem by installing standard commercial sensors in the interior of a wedge probe.

(iii) *Sensor position in cylindrical probes*. Flat diaphragms or sensor chips have also been mounted on convex surfaces such as spheres or cylinders (Kerrebrock *et al* 1980, Epstein 1985), at cost of a local discontinuity of the shape. Gossweiler *et al* (1990; figure 10) preferred a cylindric geometry and packaged four sensor chips into the probe tip. This design focused on minimizing the tip size (diameter 2.5 mm) and protecting the sensors from external damage, while ensuring a smooth probe surface with well defined tap positions. A remarkable 6 mm cylinder probe has been built by Riess and Walbaum (1994). The six sensor taps are distributed around the circumference to detect fluctuating flow from all yaw directions in an axial flow compressor during stall.

3.2.3. Packaging and sensor properties.
One main task of probe development is to find a compromise between the basic sensor properties and the sensor packaging technique— which introduces new boundary conditions regarding both temperature/pressure transient behaviour and long term stability. These issues, and in particular the impact of the miniature probe size on the sensor properties, have also been thoroughly investigated (e.g. Cook 1989, Gossweiler 1993,
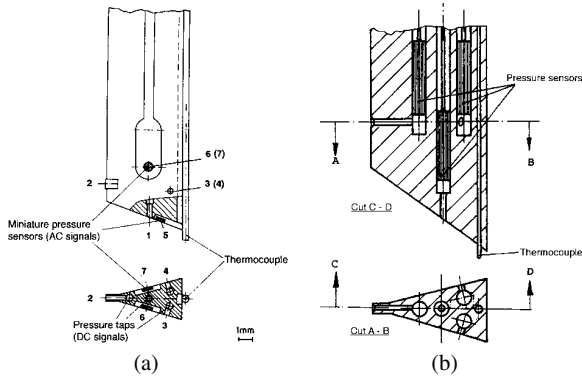
Figure 9. (a) Three-sensor probe developed by Bubeck and Wachter (1987). The total pressure sensor was given up for the sake of a smaller probe size. Therefore the probe has to be turned consecutively in two yaw positions to determine the 3D flow information. Besides the surface-mounted pressure sensors and the thermocouple at the trailing edge, additional pneumatic taps are used to provide the DC pressure signal part, on which the sensor AC information is superposed. (b) Heneka's four-sensor probe (1983) has standard commercial pressure sensors mounted within the tip.
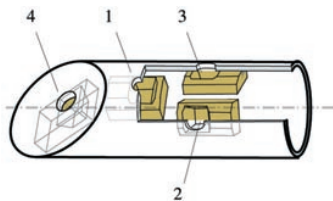

Figure 10. Tip of a fast-response cylindrical probe with four miniature pressure sensor chips (tip diameter 2.5 mm, Gossweiler 1993).

Kupferschmied 1998). New concepts allowing miniature manufacturing in small series were developed, based on micromechanics and microelectronics. A one-sensor Pitot probe featuring an outer diameter of 0.84 mm was designed by Kupferschmied *et al* (1994; figure 11) to demonstrate the feasibility and limits of these technologies. For example, tolerances of the complex miniature probe parts machined by electro-discharge have typically to be within 0.01 mm. Also, the chip bonding technique (i.e. miniature but reliable electric connections to the sensor chip) proved to be critical.

Based on these experiences, these authors developed two types of cylindrical probe with an outer diameter of 1.80 mm, accommodating one and three sensors, respectively (figure 12). A fourth sensor can be implemented into the latter probe type without increasing the diameter, enabling 3D flow measurements.

For the use in the VKI blow-down facility Brouckaert *et al* (1998) developed a fast-response probe accommodating three absolute-pressure sensors located in the same tip plane (figure 13). The cylinder-elliptic shape was chosen to increase the stiffness. An ingenious particularity of this design is the trailing edge air blowing. CFD investigations confirm that a controlled air blowing helps to stabilize the probe wake flow and thus reduce measurement errors due to time-dependent aerodynamic effects like locked on vortex shedding.

Figure 11. Tip of one-sensor Pitot probe of 0.84 mm diameter manufactured mainly by electric discharge machining (Kupferschmied *et al* 1994). The sensor chip (sensitivity of typically 90 mV bar^{-1} at 5 mW excitation power) is located one tip diameter behind the tap to improve the accuracy of the total pressure reading and reduce the angular sensitivity. The limitations were shown to be related to assembly, electric connections and sealing.
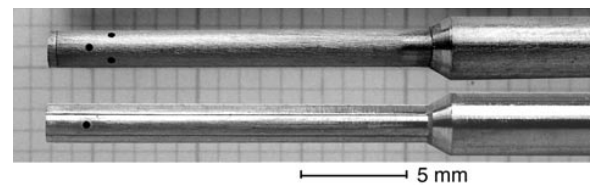

Figure 12. Tips of a one- and a three-sensor probe of 1.80 mm diameter (Kupferschmied 1998). The sensor chips are located behind the taps, as in figure 10, with the diaphragm turned towards the interior to avoid damage due to particle impact on the chip's active side. This kind of probe has been successfully operated over several hundred hours.
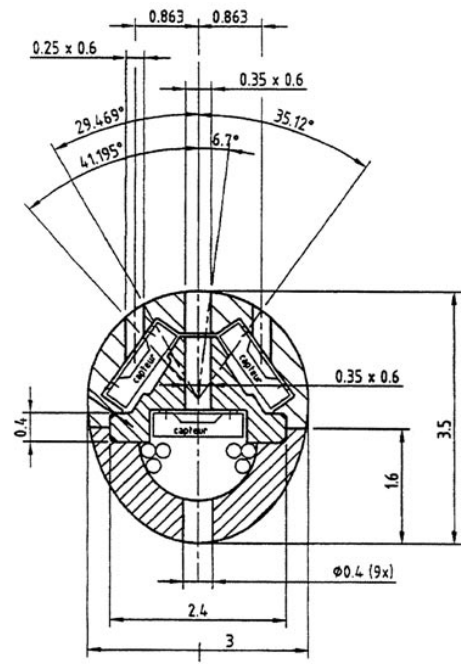

Figure 13. Cross-section view of the three-sensor probe with trailing edge air blowing developed at the VKI (Brouckaert *et al* 1998).

3.3. Access requirements

The future access to the turbomachinery flow section is also a design issue for both probe tip and shaft. The probes are

usually inserted radially through the casing at one or more positions. The bore diameter of 6 to 10 mm required is much small than the optical windows used by other measurement techniques. To further improve the operational flexibility, most fast-response probes shafts are prismatic. They are traversed by high precision probe actuators using stepping motors, either radially or axially. Traverses in circumferential direction are possible as well but generally require a special design of that casing area.

4. Calibration requirements and procedures

Basically, fast-response probes have to undergo two calibration steps prior to their application—the voltage calibration of the sensors as a function of temperature, pressure and time and the aerodynamic calibration of the probe in a reference flow.

4.1. Sensor calibration

Depending on the time duration of probe usage considered, different sensor properties are of interest:

(i) *Static properties.* What is the achievable DC (steady state) accuracy of the pressure and temperature measurement? What are suitable time intervals before the sensors have to be recalibrated (long-term properties)?

(ii) *Transient properties.* What is the transient response of the pressure and the temperature reading? How do temperature transients affect the sensor properties?

While it is reasonable to calibrate the sensors under static conditions prior and after each application, the behaviour under dynamic conditions—i.e. in fast temperature or pressure gradients—is complex and is usually limited to investigations for specific probe types only.

4.1.1. Static pressure and temperature calibration.
In order to map the sensor characteristics over the whole pressure and temperature range expected in the measurements, the sensors are submitted to stepwise varied temperature and pressure. As this process lasts generally many hours, this 'static' calibration is often performed in automatic facilities, consisting of an environmental chamber in which the temperature can be accurately controlled. Pressure steps are applied either by varying the pressure level of the probe interior for differential pressure sensors or by changing the pressure in the environmental chamber for absolute pressure sensors.

Turbomachinery applications revealed much interest for accurate flow temperature information obtained by using the same probes as used for flow velocity measurement. Piezoresistive sensors are sensitive to pressure and temperature as well, and the sensor calibration links both types of datum to voltage values. While the offset of each pressure signal can be readjusted during measurements by changing the reference pressure in the probe interior, a temperature offset cannot easily be detected while the probe remains inserted in the machine. Therefore, stability of the temperature reading is a requirement.
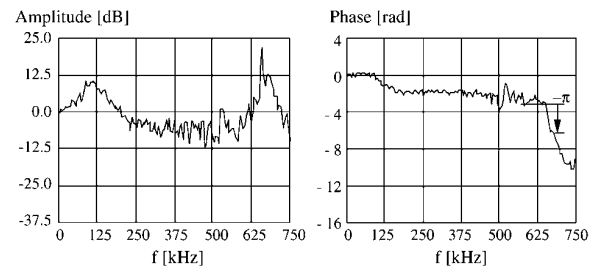

Figure 14. Amplitude and phase response of a miniature pressure sensor in a recessed cavity determined in a shock tube (Gossweiler 1993). The first peak reveals the natural frequency of the cavity (90–105 kHz, depending on the probe type), and the second peak the sensor diaphragm eigenfrequency (650–850 kHz, depending on sensor type).

Due to the excitation power dissipated in the sensor's resistors, the sensor diaphragms are prone to overheat, whereby the measured absolute temperature level as well as the pressure signal stability are affected. Epstein (1985) reported a sensor overtemperature of 20 to 30 K when the probe was in still air at ambient temperature. He then equipped his probes with a cooling system. However, a cooling is not only problematic for the probe design (size and reference pressure supply), but also prevents the measurement of temperature.

The overheating ΔT of cylindrical probe tips was shown to be strongly dependent on the sensor excitation current and also the tip size (Kupferschmied *et al* 1998). It must be accounted for if the probe is used for flow temperature measurements as well.

4.1.2. Dynamic sensor calibration.
Basically, the dynamic response of the pressure signal depends on the dynamic properties of the sensor diaphragm and its distance to the source of pressure fluctuations. For flush mounted sensors (figure 9(a)) the frequency response is mostly dictated by the natural frequency of the diaphragm. If the membrane has a silicone rubber protection coating, the natural frequency is modified by the additional mass (Gossweiler 1993). The diaphragm of internally mounted sensors is recessed from the pressure tap (see figure 10) and thus forms a pneumatic cavity which alters the dynamic response of the pressure signal (figure 14).

Although analytical approaches with simple models such as organ pipe, Helmholtz resonator or even the 1D theory of Bergh and Tijdeman (1965) provide a valuable estimate of the cavity's resonance frequency, they tend to overestimate the reality by a factor of 1.5 to 2, due to 3D effects in the cavity. Depending on the accuracy required in terms of analogue bandwidth, amplitude and phase, an individual calibration of each probe should be envisaged. A numerical correction of both amplitude and phase response can then be applied to the time series during the measurement data processing.

The behaviour of the pressure and temperature signals under small and large temperature gradients—e.g. occurring during the run-up of a turbomachine or the sudden immersion in hot flows—should be tested for each probe type. A typical response of the indicated pressure zero is presented in figure 15 (left) during a gentle temperature change (maximum
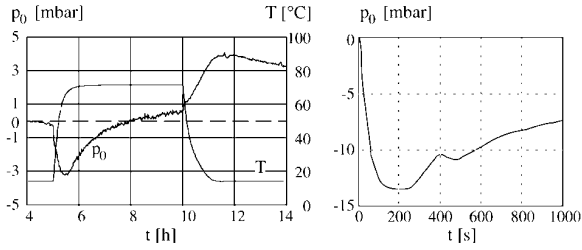
Figure 15. Indicated pressure zero after temperature changes of ±60 K and after a step of +60 K (probe FRAP C1S18 No 12). The response of the indicated temperature shows a first order system behaviour, with a time constant $\tau_{63\%}$ of 13.8 s for this one-sensor probe type in low air velocity (1.5 m s^{-1}). The shorter time constant of 7.5 s of the three-sensor probe type C3S18 (not shown here) is due to the completely different design of the tip interior. The time constants decrease roughly by an order of magnitude if the flow velocity is increased to $M = 0.5$ (other conditions unchanged).
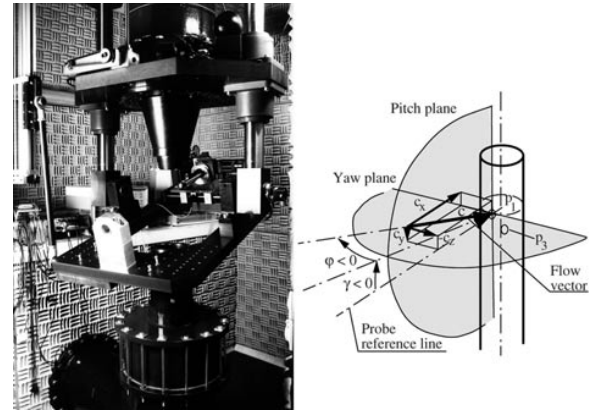

Figure 16. Left: vertical-nozzle free jet facility (diameter 100 mm) of the ETH Turbomachinery Laboratory. This dedicated facility has been designed to achieve an accuracy one order of magnitude higher than the accuracy required in the later application.

Right: probe frame of reference: yaw–pitch system as defined by Treaster and Yocum (1979).

4 K min^{-1}), and in figure 15 (right) for a sudden temperature step of 60 K.

The time constant of the indicated temperature (1 s at $M = 0.5$) confines such probes to mean flow temperature measurements. Other techniques like aspirating probes or cold wire probes are necessary for time-resolved temperature measurements in turbomachinery (e.g. Ng and Epstein 1983, Arts *et al* 1996).

4.2. Aerodynamic probe calibration

4.2.1. Calibration in steady reference flow.
The probes have to be aerodynamically calibrated for several Mach number steps meeting the conditions expected in the application. This can be done either in an open jet facility (figure 16) or in closed wind tunnels, especially in the case of transonic flows. Due to the inherent flow unsteadiness fast-response probes must cover large angular ranges with a fine resolution. Therefore, meshes with several hundred combinations of probe yaw and pitch angles are necessary for each probe at any Mach number level. To make these time-consuming calibrations feasible, such a calibration system is generally fully computer controlled and achieves typically some 600 to 1000 angular positions per hour with fast-response probes.

Typical non-dimensional pressure coefficients C_p determined in the jet nozzle for each tap of the cylindrical three-sensor probe seen in figure 12 are shown in figure 17.

4.2.2. Calibration in unsteady flows.
Although a calibration in controlled dynamic flows would be very valuable, no facilities are available yet to provide such reference conditions in air for turbomachinery relevant frequencies. Therefore the time-dependent part of the probe aerodynamics has to be investigated at low frequencies with large-scale models either in water (Humm *et al* 1994) or in air (Ainsworth *et al* 1995) and the results transferred to real-size applications by using model laws.

4.2.3. Calibration of the temperature.
To prepare the probes for measuring the (time-averaged) flow temperature
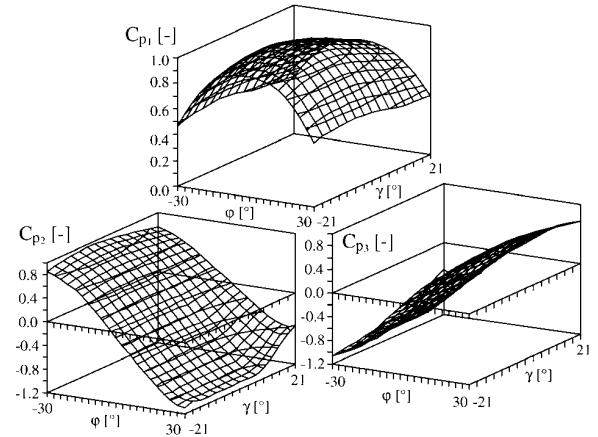
Figure 17. Aerodynamic coefficients of a three-hole probe (C3S18P, diameter 1.80 mm, $M = 0.30$). Each mesh node is a calibration point. The frame of reference of the probe is defined in figure 16 (right). The overall repeatability of the C_p is better than ±2%.

besides the time-resolved pressure, these must be calibrated for static temperature in terms of Mach number and flow angle. The difference between the total flow temperature and the temperature indicated by a one-sensor probe is plotted in figure 18 for two typical yaw positions of the probe (stagnation point and angle where the static pressure is measured at zero yaw). A corresponding 'effective recovery factor' shown in figure 19—which accounts for the external heating by flow friction and the heat conduction in the probe interior—has been defined here by using the nozzle velocity c_F and the specific heat c_p as:

$$r = 1 - \frac{2c_p}{c_F^2}(T_{tot} - T_i).$$

4.3. Processing of calibration data

4.3.1. Modelling of sensor calibration data.
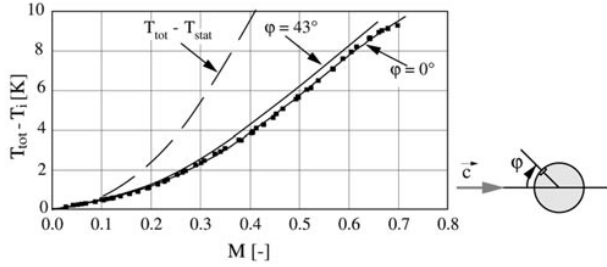As mentioned in section 3.1.1 the solution using electronic

Figure 18. Difference between the flow total temperature and the temperature indicated by the probe FRAP C1S18 No 12.
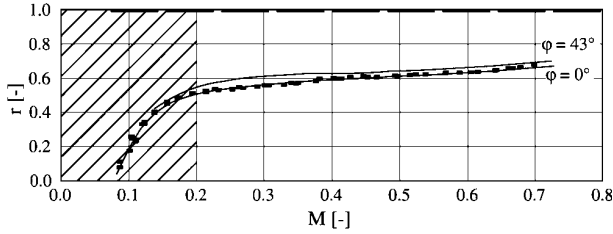

Figure 19. Probe temperature coefficient of the probe FRAP C1S18 No 12 in air at ambient temperature (yaw angle $\varphi = 0°$; $T = 24\,°C$). Whereas the dashed line $T_{tot} - T_{stat}$ in figure 18 illustrates the Mach dependency of the adiabatic flow temperature rise at the stagnation point, the real 'effective recovery factor' of this type of probe (solid lines with or without data points) lies around 0.6. This much lower value is due to heat conduction in the probe interior. Due to its definition, the uncertainty of r increases strongly for low velocities where the temperature head $T_{tot} - T_{stat}$ is low (shaded range).

circuits to compensate temperature effects tends to be replaced by numerical approaches (e.g. model-based reconstruction by Gossweiler *et al* 1990). Selected sensor data collected during the static calibration (U, $U_e = F(\Delta p, T)$, see figure 6) are approximated with the following polynomial model after an exchange of the dependent and independent variables:

$$\Delta p(U, U_e) = \sum_{i=0}^{m} \sum_{j=0}^{n} k_{p_{ij}} U^i U_e^j$$

$$T(U, U_e) = \sum_{i=0}^{m} \sum_{j=0}^{n} k_{T_{ij}} U^i U_e^j.$$

The approximation method enhances the accuracy remarkably and reduces also the complexity of calculations. In most cases, polynomials with $m = n = 2$ satisfy the accuracy requirements (Kupferschmied *et al* 1999).

4.3.2. Modelling of probe calibration data.

Basically, the methods used do not differ from conventional pneumatic probes (e.g. Bohn and Simon 1975), apart from the larger angular ranges required by fast-response probes. The aerodynamic calibration coefficients C_p obtained for every probe pressure tap are combined into an appropriate set of non-dimensional aerodynamic coefficients to allow the evaluation of the physical flow quantities from the pressure readings. The choice of these coefficients mainly depends upon the probe geometry and the data processing method. For example, the coefficients proposed by Krause and Dudzinski

(1969) with yaw and pitch sensitivities K_φ and K_γ are widely used (see also figure 16 right):

$$K_\varphi = \frac{p_2 - p_3}{p_1 - p_m} = K_\varphi(\varphi, \gamma, M) \qquad \text{with } p_m = \frac{p_2 + p_3}{2}$$

$$K_\gamma = \frac{p_1 - p_4}{p_1 - p_m} = K_\gamma(\varphi, \gamma, M).$$

Note that K_φ and K_γ are non-dimensional numbers defined by the pressure sensor readings. The total and static pressure sensitivities are given by

$$K_{tot} = \frac{p_{tot} - p_1}{p_1 - p_m} = K_{tot}(\varphi, \gamma, M)$$

$$K_{stat} = \frac{p_{tot} - p_{stat}}{p_1 - p_m} = K_{stat}(\varphi, \gamma, M).$$

If φ, γ and M are known, these equations yield directly p_{tot} and p_{stat}. Since all coefficients also depend on the Mach number, the calibration has to be performed for several Mach number steps and interpolated. In the Reynolds number range often encountered ($\mathrm{Re}_S \cong 10^{-3}$–$1.2 \times 10^5$), viscosity effects only have a marginal influence for this probe geometry, making a variation of Re unnecessary. Further, the angular range in which data can be evaluated is limited by the value of the denominator $p_1 - p_m$, which shows numerical poles at large angles.

To allow the more efficient direct (i.e. non-iterative) evaluation of massive amounts of measurement data, the dependent and independent variables of the calibration coefficients K_φ and K_γ are exchanged according to:

$$\varphi = F(K_\varphi, K_\gamma) \qquad \text{and } \gamma = G(K_\varphi, K_\gamma).$$

The calibration surfaces represented by these equations, see e.g. figure 20, can be approximated with bivariable polynomials. The Mach number is iteratively taken into account by using an interpolation between the discretely calibrated M steps. The degree of the polynomial depends on both required angular range and desired accuracy. Practical limits for the degree are set by the CPU time and by the number of data points available (a high degree of freedom is required for the least-squares approximation to avoid numerical oscillations). The residuals of the angle evaluation of the four-hole probe are shown in figure 21 when the calibration data are modelled to different degrees m, n and within different angular ranges.

5. Data processing—conversion and analysis of time-resolved data

Time-resolved measurements produce a massive number of data that have to be processed accordingly. A campaign in the ETH radial compressor test rig 'Rigi' provided e.g. more than 280 million data points. The processing of these data has to consider different requirements such as the handling by appropriate software programs, the conversion of the voltage signals into flow quantities, the application of phase averaging and the adequate presentation of the results. Furthermore, special traverse concepts may become
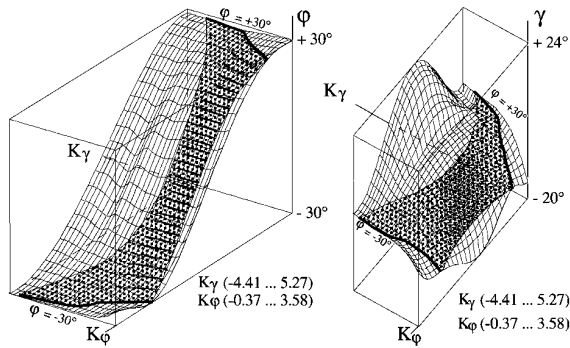
Figure 20. Calibration surfaces φ (K_φ, K_γ) and γ (K_φ, K_γ) of a cylindrical four-hole probe at $M = 0.2$ (Kupferschmied 1998). Due to the large angular range required for fast-response measurements, the coefficient surfaces show a rather complicated shape.
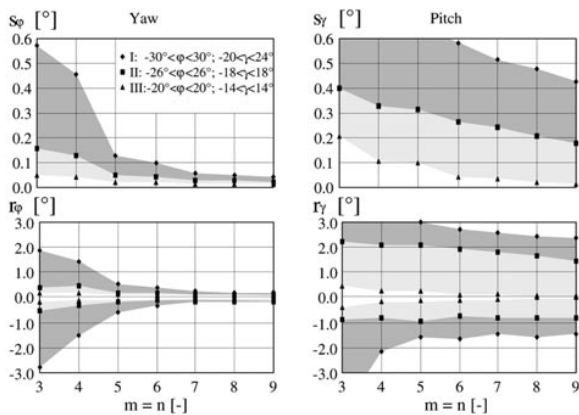

Figure 21. Accuracy of the yaw and pitch angle evaluation model depending on the polynomial degree ($m = n$) and three different angular ranges I, II, III (same probe as in figure 20). Here, polynomial degrees $m = n = 6$ are a good compromise: the standard deviation of the yaw residuals remains within $0.1°$ for all three angular ranges. The residuals of the pitch angle are more sensitive to the angular range ($0.05° < r_\gamma < 0.6°$). The extreme residuals (figure 21, bottom) are not only influenced by stochastic calibration errors, but also by systematic differences in some regions of the surfaces.

necessary for measurements in unstable operation to take into account particular flow conditions.

To compare time-resolved flow quantities such as velocity or flow angle history with time-mean data measured with pneumatic probes, data averaging is necessary. Different averaging methods are available as time averaging, physical meaningful (conservation-law based) averaging or mass flow weighted averaging. Figure 22 shows the time-averaged flow angle variation across the flow channel at the exit of the impeller. To obtain the time-averaged quantities at any traverse position nearly a million sensor pressure values were measured, converted into flow angle values and time averaged to give the black dots shown. For two dots a short part of the time series (about 0.5% of 200 000 points) is displayed in the plot.

The example in figure 22 illustrates the amount of information contained in time-resolved data. The objective of data processing is to reveal flow effects with focus on the goals of the measurement campaign. Shreeve *et al*
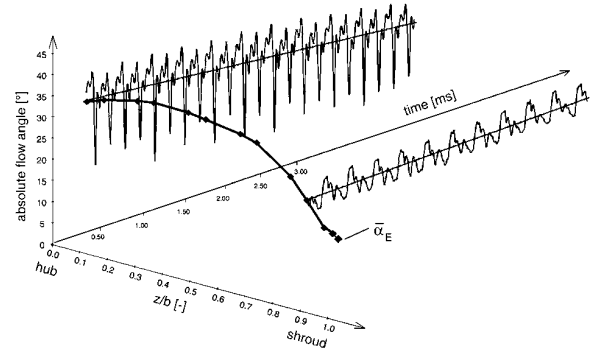

Figure 22. Example: Compression of the time-resolved absolute flow angle α_E into the time-averaged distribution of $\bar{\alpha}_E$ over a wall-to-wall traverse.

(1978), Lakshminarayana (1981), Capece and Fleeter (1989), Larguier (1985), Belhabib and Miton (1985), Dambach and Hodson (1999) and many other authors reported on data processing or data reduction with regard to time-resolved measurement. Relevant topics of data processing comprise

(i) goals and planning of measurement campaigns, which should guide the data processing;
(ii) measurement concepts optimized for data analysis procedures;
(iii) data conversion from voltage sequences into flow quantity sequences;
(iv) data analysis (averaging, statistics, . . .) and
(v) software programs with graphic processing tools.

5.1. Measurement concepts from the point of view of data processing

The measurement concept must define the probe type and traversing concept (including the measurement grid and the length of measured data samples) and must harmonize the measurement system with the key data of the machine; e.g. in the case when several probes are simultaneously used at several locations, the traversing strategy must include all probes.

5.1.1. Different probe types. Single or multi-sensor probe types can be used. Depending on the number of sensors in the tip of the probe the velocity in the flow can be measured as a 3D or as a 2D field only (see table 3). The velocity can be determined in three dimensions with a four-sensor probe and all flow quantities such as total pressure, static pressure, yaw and pitch angle are fully time resolved. The disadvantage is the larger measurement volume given by the four sensors placed in the tip of the probe. The complexity for the measurement system increases strongly.

A cylindrical one-sensor probe used in a 'pseudo-three-sensor' mode has a small measurement volume: at every traverse position the fluctuating flow is measured time resolved under three angular positions of the probe shaft while the machine is running at constant conditions. The middle one of the three angle positions should approximately be set to the time-averaged flow direction at the local position. For the other two angle positions the probe is rotated (in yaw) by $\pm 43°$. A once per revolution signal from a trigger is used

Table 3. Different probe types and operation modes and their limitation with respect to the resolution of the velocity field.

	Four-sensor probe	Three-sensor probe	One-sensor 'pseudo three-sensor' mode	Two one-sensor probes 'pseudo four-sensor' mode
Velocity	3D	2D	2D	3D
Flow quantities	time resolved	time resolved	only phase averaged	only phase averaged
Measurement volume	large	medium	small	small
Complexity	high	medium	small	small

to combine the sensor signals to a quasi-synchronous pseudo-three-sensor probe. (For a pseudo-four-sensor probe the same procedure is applied with two probes having one sensor each or one probe having two sensors.) The first solutions, using two one-sensor probes, give the possibility to reduce the tip diameter because only one sensor has to be fitted into each tip. The disadvantage is the need to repeat each traverse with a second probe. The advantages of using one-sensor probes in the pseudo three-sensor or pseudo four-sensor mode are

(i) Only one sensor has to be controlled during the measurements.

(ii) The probe construction is simpler and the production costs are lower. Also the probe diameter can be made smaller.

(iii) Only one amplifier, one A/D converter and fewer electric connections are necessary. This reduces the system complexity and the potential for errors.

(iv) Only stochastic measurement errors from one sensor must be considered in the flow quantities.

(v) The flow quantities measured in a turbomachine have to be phase averaged anyway in order to separate stochastic and deterministic fluctuations.

(vi) Even though no time correlated 'true' turbulence information is available, the turbulence intensity can be qualitatively determined as shown by recent comparisons between one-sensor probes and LDV measurements, see Köppel (2000).

In general, the choice of the probe type will of course depend on the goals of a measurement campaign.

5.1.2. Traversing concepts. The traversing concepts are strongly dependent on the flow effects to be detected. An example is backflow during rotating stall running conditions in the centrifugal compressor Rigi (see figure 25 further below) where the flow direction may fluctuate over a full 360 degrees. The maximum yaw angle range of a cylindrical probe calibration model is about $\pm 35°$. Therefore the probe was turned into as many as 11 yaw positions at each traverse position in order to simulate ten pseudo three-sensor probes over a yaw angle range of $\varphi = 360°$. Between each yaw angle position there was a difference of $43°$ that corresponded to the position of three sensors in the simulated three-sensor probe. The main issues concerning the planning of probe traverses are:

(i) Number of running conditions and geometry variations to be investigated, and number of traverses in each case.

(ii) *Number of traverses.* Behind rotors a single traverse is normally sufficient, if the space between stators

and rotors is broad enough to let blade-to-blade non-uniformities be reduced. Behind stators, there is often the need to make several traverses along lines displaced along the circumference over one stator pitch, in order to see the influence of the stator's potential field and to explore stator blade boundary layers and wakes. In the case of clocking investigations (interaction between stator and next stator or rotor and next rotor) several traverses are necessary behind a rotor row in circumferential direction.

(iii) *Number of yaw positions.* Using single-sensor probes more than three yaw positions are necessary in backflow conditions, and the time-resolved data have to be always conditionally averaged to link all measurements together.

(iv) *Number of traverse points.* To resolve high gradients the traverse points have to be closely spaced. The traverse points should preferably be on the same stream surfaces for measurements in front and behind a stage.

(v) *Number of sensor offset and gain adjustments.* The number of adjustments per traverse depends on the measurement time at one yaw position, the sampling frequency and the storage capacity. More adjustments help to increase the accuracy.

5.1.3. Key machine data and characteristic data of the measurement campaign. The third part of the measurement concepts treats the parameter choices associated with the objectives of a measurement campaign and with the key data of the compressor.

In figure 23 the key machine data and the characteristic data of the measurement system are shown at the example of the measurement campaign in the centrifugal compressor Rigi during best point running conditions, see section 6.2.

5.2. Data conversion

The steps required to convert probe voltage data into flow quantities are summarized in figure 24. The sensor voltages have been converted into pressure and temperature signals with a model based reconstruction using sensor calibration coefficients, see section 4.3.1. The flow angles are determined via the yaw and pitch sensitive coefficients. The total pressure and the static pressure are calculated from the flow angles. The other quantities such as flow velocity, Mach number and temperature are computed later on.

5.3. Data analysis

While data conversion is a necessity for all probe techniques, data analysis is an optional step facilitating the interpretation

Key data of the machine		key data of the measurement campaign	
Impeller RPM	17720rpm	Number of points per traverses for BP	13
Number of Blades z_B	22	Number of data points between 2 blades	31
Blade passing frequency: $f_{Bp}=z\, f_{Rmax}$	$f_{Bp} \approx 6.5$kHz	Sampling frequency f_A for „best point"	200 kHz
Other important frequencies	$f_{MildSurge}=18$Hz $f_{RotatingStall}=42$Hz	Data length (measuring time)	163840 points (0.82s)
		Number of revolutions per averaging	242
		95% confidential interval for ensemble averaging	$a = 7.9$mbar $a/\sigma=7.9/63=$ 0.1
Dynamic head	≈220mbar	Accuracy of the sensor (signal/noise ratio)	220/0.07 = 3142 70dB
		Sensor sensitivity	6.3mV/mbar
Max. pressure peak Averaged pressure	2200mbar 1510mbar	Reference pressure in the probe shaft (absolute)	1700mbar
Max. pressure fluctuation	Max: 814mbar (peak to peak)	Range of the voltage signals from sensor	±5 V for U ±10 V for Ue
		Resolution of the sensor pressure signals for ±5V	0.4 mbar (12 bit)
Max. angle fluctuation	$\Delta\varphi$= 16.6°	Calibration range of the yaw angle	φ= ±20°
Mach number	0.75	Calibration range of the Mach number	0.2 < M < 0.7
Max. temperature	62.1°C	Number of offset and gain adjustments	2 per traverse
		Spatial resolution of the probe (d_{Probe})	d_{Probe} =1.2mm
Spatial dimension of a fluid part ($f_{Bandwidth}$=44kHz)	d_{fluid}=4.4mm (c_{max}=192m/s)	Max. resolution of frequency ($f_{max}= c_{max}/d_{Probe}$)	f_{Max}=160 kHz (c_{max}=192m/s)
Stability of the machine at the operating point (BP)	678 ± 1 measuring point per revolution	Minimum resolution of the frequency determined from spectra density	f_{Min}=100Hz

Figure 23. Key data of the measurement campaign at the best point of the ETH radial compressor 'Rigi' with reference to the measurement objectives and the characteristic data of the compressor (Köppel *et al* 1999). In the upper part the dominant frequencies of the compressor and the key data of the measurement grid are listed. In the middle part on the left side the maximum expected values of the compressor flow quantities are shown. On the right side the resulting parameters of the measurement system, the resolution of the sensors and the calibration range limits are noted. In the third part an estimation of the length scales of turbulence and the spatial resolution of the probe are given. The measurement grid is determined by the number of traverse points and by the number of samples between the passage of two blades, which is defined by the rotational speed of the machine, number of blades and the sampling frequency. The average magnitude of the dynamic head of 200 mbar leads to a high signal to noise ratio of 70 dB. This means that the full dynamics of the measurement electronics (here 72 dB) could be utilized.

of data. The main topics of data analysis are:

 (i) conversion of flow quantities;
 (ii) averaging;
(iii) statistical analysis;
(iv) frequency analysis and
 (v) graphical processing.

Converted flow quantities can be e.g. the relative velocity measured at the exit of rotor, the enthalpy or the efficiency over a stage. All flow quantities build the base of data analysis. The averaging methods compress the data and are ideal to obtain a fast overview about the flow quantities. Data averaging is also necessary if a one-sensor probe is used in a pseudo three-sensor or four-sensor mode to link the time series obtained. The statistical part of data analysis yields standard deviation, higher moments, functions of correlations and confidence tests.

The frequency analysis focuses on the fluctuations in the flow. Of primary interest are the fluctuations
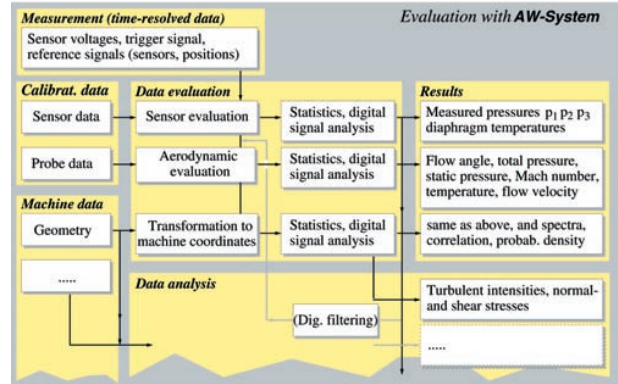

Figure 24. Steps of the conversion of measured data.

associated with the blade passing frequency. These reveal many details of stator secondary flows, wakes, leakage and cooling streams etc. Under particular running conditions in turbomachinery, however, several characteristic flow fluctuations are superposed. For example, the characteristic fluctuations during rotating stall in a centrifugal compressor are produced on one hand by the passing of blades and on the other hand by the propagation of the stall cell. In this example power spectra, digital filters and statistical functions (e.g. standard deviation) are applied to identify the frequency of a rotating stall cell. Further the separation of deterministic and stochastic or other important frequencies gives additional understanding of the intensity of specific fluctuations (e.g. Evans 1975, Binder *et al* 1989, Sentker and Riess 1996). The determination of turbulence intensity is also part of the frequency analysis in turbomachinery flows.

One important aspect of data analysis that should be considered in more detail in this contribution is the averaging of time-resolved data. The other topics of data analysis such as turbulence measurement with fast-response probes or the application of statistic procedures are described in detail in Köppel (2000).

5.3.1. Averaging methods. Phase averaging (ensemble averaging) methods compress the time-dependent information, while conserving the character of fluctuations associated with a particular frequency (e.g. blade passing), see Bendat and Piersol (1991), Gostelow (1977) or Shreeve and Neuhoff (1984). In modulated flow, phase averaging has to be based on the time period of the phenomenon to be studied—e.g. the shaft revolution period or the period of mild surge or rotating stall.

In the first case triggering can be done by a geometric signal like a rotor or a blade. The period length is almost constant. This rotor-based phase averaging can be applied under stable running conditions of a turbomachine where the rotor frequency is constant. The rotor-synchronous frequency can be separated from the non-synchronous which is often a measure of turbulence. The separation of deterministic and stochastic fluctuations is interesting to understand aerodynamic loss mechanisms.

In the second case the trigger is independent of rotor revolutions and has to be based on an event-related flow condition. Such trigger signals usually have variable period

length and the number of measured data obtained between two trigger events is not constant. A period-related 'class averaging' method has to be used, as described e.g. in Roduner *et al* (1999b). The number of classes determines the resolution in time and the statistical accuracy of the averaging process. Specific fluctuations of a flow phenomenon can be separated from the blade passing fluctuations.

Physically correct averaging methods are relevant from the point of view of turbomachinery theory. The averaging procedure strictly respects the conservation laws (of mass, momentum and energy) and the average values are suitable for the mass, force and energy balances. Traupel (1982), Dzung (1967), Adamczyk (1986) and Kreitmeier (1987) reported about such averaging methods. In Köppel *et al* (1999) the averaging methods of Traupel and Dzung have been applied to data from fast-response aerodynamic probe measurements. Physically correct averaging is imperative for efficiency calculations.

5.4. Software for data processing

The requirements toward a data conversion and analysis software are described with reference to the FRAP system. Three important topics for such a software are:

 (i) graphical user interface;
 (ii) reading and processing of huge data arrays and
 (iii) graphical processing of the evaluated and calculated results.

A measurement campaign comprising only five traverses with 15 points each produces more than 300 files which have to be handled by the software. Furthermore, all file names pertaining to calibration data, all information on settings and machine specific data have to be considered. The graphical user interface helps to link all file names in the right order. The graphical processing of the results is required for the interpretation of all measured effects. In the case of the FRAP evaluation and analysis software the graphical processing is designed to be interactive, giving the user the possibility to surf through the results.

6. Fast-response probe applications

6.1. Introduction

Over the last decades, important time-resolved flow information in turbomachinery has been gained using the fast-response probe measurement technique. An overview of some published examples of applications is given in table 4. Some more references and details are provided in reviews by Gossweiler (1996) and Sieverding *et al* (2000).

In order to illustrate some of the possibilities offered by this technique, examples of results from measurements with the ETH FRAP system in a centrifugal compressor facility are presented in the following sections, with emphasis on:

 (i) assessment of the DC accuracy by comparing time-resolved results with results gained from conventional pneumatic probe and standard orifice measurements;
 (ii) comparison with LDV measurement results and
 (iii) measurement and data processing of rotating stall with a fast-response one-sensor probe.

Table 4. Overview of some published work using fast-response probe applications in turbomachinery.

| Author(s)		Application
Kerrebrock *et al*	1974	Transonic axial compressor
Eckhardt	1975	Centrifugal compressor impeller exit
Shreeve *et al*	1978	High speed axial compressor flow
Shreeve and Neuhoff	1984	
Heneka	1983	Cold axial turbine
Larguier	1985	Axial compressor exit
Ng and Epstein	1985	Transonic axial compressor
Bubeck and Wachter	1987	Axial compressor
Ng and Popernack	1987	Kármán vortex shedding and air jet
Cook	1989	HP axial compressor
Cherrett *et al*	1995	Transonic fan rotor exit
Roduner *et al*	1999a	Centrifugal compressor
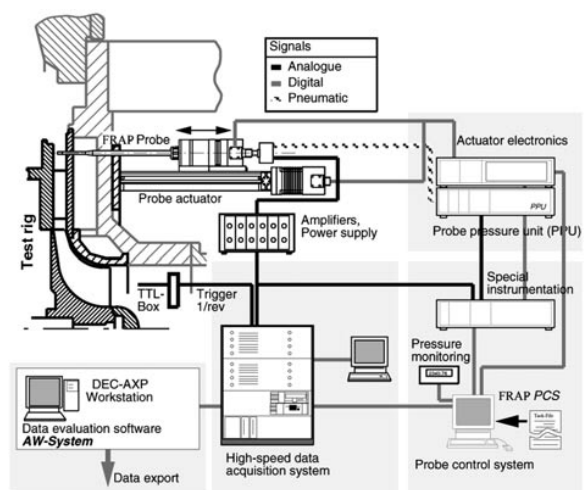
Figure 25. Configuration of the fast-response probe measurement system (ETH FRAP) used in a centrifugal compressor.

6.2. Measurements in a centrifugal compressor

The stage consists of an unshrouded impeller of 22 blades where 11 of them are splitter blades. At the exit the blades have a back lean of $30°$ to the radial. The impeller is followed by a vaned diffuser with two parallel walls and 24 prismatic, circular-arc vanes. The test rig and set-up of the measurement system are described in detail in Roduner *et al* (1999a, b) and in Roduner (1999). Figure 25 shows the measurement system configuration for these measurement campaigns in this test rig.

Wall-to-wall probe traverses were performed at the exit of the impeller at a radius ratio of $r/r_2 = 1.05$. Probe traverses were performed under design running conditions as well as under off-design conditions.

6.3. Comparison of probe measurements

Investigations aimed at quantifying the accuracy of the DC part of the signal were performed first. Results of conventional pneumatic probes and FRAP probes were compared. Additionally, the mass flow measured with the standard orifice of the test rig and that calculated from FRAP probe traverses were compared (for details see Roduner *et al*
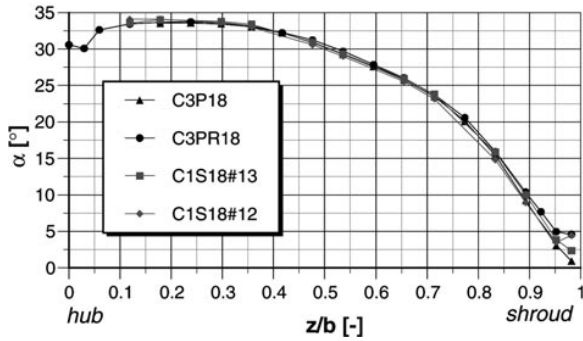
Figure 26. Wall-to-wall flow angle distribution at $r/r_2 = 1.05$, measured with two different pneumatic probes (black) and two FRAP probes (grey).

Figure 27. Wall-to-wall dynamic head distribution at $r/r_2 = 1.05$.

1999a). To verify the time-resolved (AC) results of the fast-response probes, the measurements were compared with LDV measurements (see Gizzi *et al* 1999).

6.3.1. Comparisons with pneumatic probes. The same measurements at the exit of the impeller were performed with four different probes. The running conditions of the stage were set to an impeller tip Mach number of Mu = 0.75 (corresponding to 17 720 rpm); the flow rate was set to the best point. All probes used were cylindrical with a tip diameter of 1.8 mm. Two were conventional pneumatic three-hole probes (C3P18, C3PR18) and two were fast-response one-sensor probes (C1S18 Nos 12, 13).

In figure 26 the flow angle distribution obtained is plotted over the diffuser width. The time-resolved FRAP probe measurements are time averaged. For the most interesting zone ($z/b = 0.1$ to 0.9) the differences are below 0.75°. Measurements above $z/b = 0.9$ are uncertain due to the horseshoe vortex created by the probe at the probe shroud–wall intersection. The flow angle differences are not systematic with respect to the pressure measurement technique used.

The dynamic head profiles measured by the four probes are plotted in figure 27 and show an identical character over the channel for all probes. C1S18 No 12, C1S18 No 13 and C1P18 gave closely identical values, too. Therefore it can be concluded, like for the steady flow measurements, that no clear difference between the two measuring techniques can be observed.

The systematic offset of the pneumatic three-hole probe C3PR18 is due to a different blockage and calibration correction (see Roduner *et al* 1999a)

6.3.2. Comparisons with orifice mass flow. The mass flow can be calculated from probe traverses by integrating the radial velocity component distribution. The main motive for doing this was comparison with the standard orifice measurement in order to check the overall accuracy of the probe traverses made.

The influence of measurement errors arising in various flow quantities derived from the probe measurement on the calculated mass flow are shown in figure 28. The mass flow measurement with probe traverses is particularly sensitive to uncertainties of the flow angle. An error in static and/or
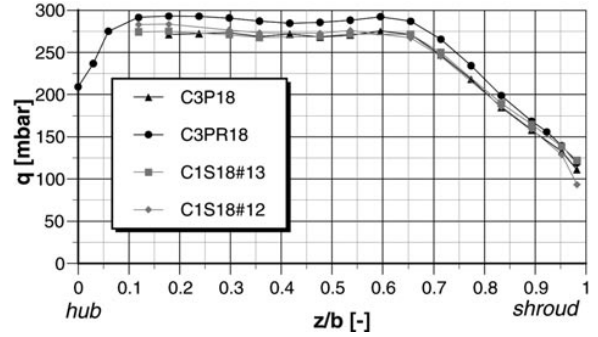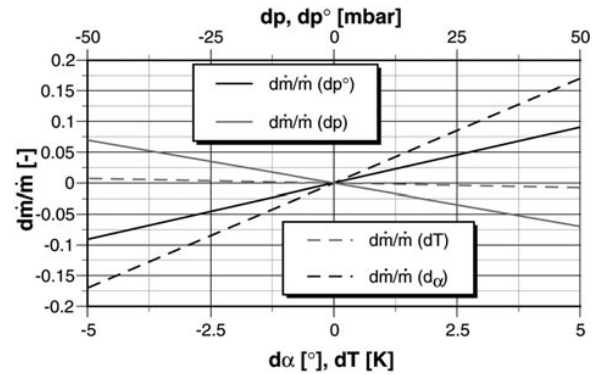

Figure 28. Effect of measurement errors of mass flow calculation.

Table 5. Comparison of mass flow calculated from probe traverses and standard orifice measurements at three different flow rates, Mu = 0.75. ($\varphi = 0.0767$ is the best point.) The C1S18 No 12 probe was used.

Flow rate φ (m)	0.0945	0.0767	0.0555
$\dot{m}$ of the standard orifice (kg s^{-1})	2.20	1.76	1.26
$\dfrac{\dot{m}_{probe} - \dot{m}_{orifice}}{\dot{m}_{orifice}}$ (%)	1.2	−0.4	−3.2

total pressure measurement leads to an error in the flow velocity magnitude. Compared to these errors, the effect of temperature errors can be neglected. A very high accuracy with respect to flow angle, static and total pressure is required to obtain the mass flow with a measurement uncertainty of 0.01 or better.

The comparisons of the mass flow calculated from probe measurements and from the standard orifice are presented in table 5. The comparisons are shown for three different flow rates, best point ($\varphi = 0.0767$), maximum flow rate ($\varphi = 0.0945$) and minimum stable flow rate ($\varphi = 0.0555$) at Mu = 0.75. For all three running conditions the mass flow rate is captured reasonably well by the probe measurements. This indicates that the fast-response probe provides accurate DC measurements.

6.3.3. Comparisons with LDV measurements. Measurements with a LDV system (see Stahlecker and Gyarmathy 1998) have been performed at the same diffuser position under identical running conditions of the stage as for the one-sensor probe traverses. The measurements were carried out at the impeller exit at a radius ratio $r/r_2 = 1.05$.
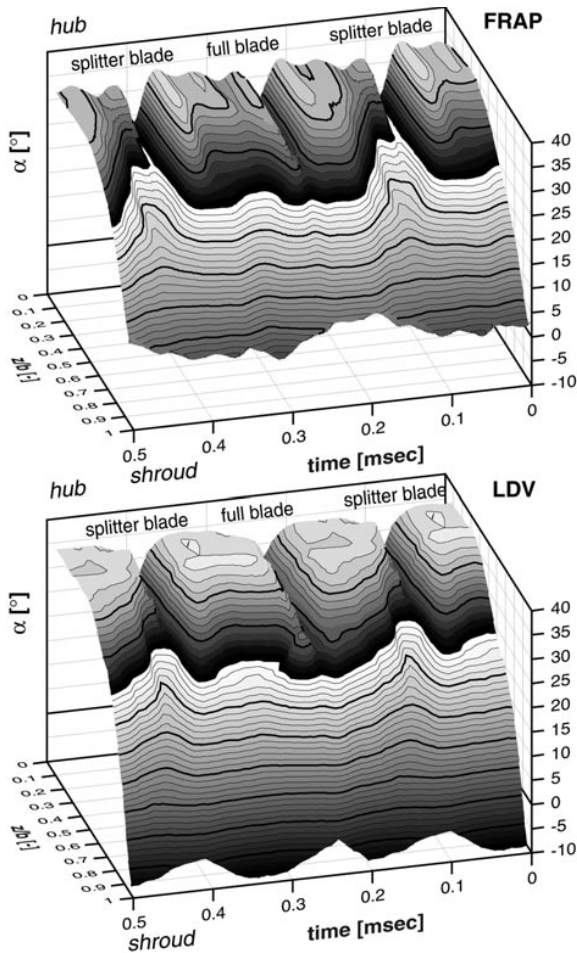
Figure 29. Comparison of the ensemble-averaged flow angle distribution at the impeller exit, measured with fast-response probes (top) and LDV (bottom); running conditions of the stage: Mu = 0.75, best point.

The compressor was operated at best point for this rim speed (Mu = 0.75, flow rate $\varphi = 0.0768$).

For comparison of blade-to-blade flow distributions, impeller revolution ensemble averaged data are presented first. Flow angle distributions from hub to shroud over the circumference are plotted in figure 29 (the flow angle α is measured to the tangent). At the top the passage of three impeller blades measured with a FRAP probe are shown. Below, equivalent data acquired by the LDV system are presented.

The following flow characteristics can be seen:

(i) The most apparent feature is the existence of a radial momentum deficiency near the shroud ($z/b > 0.8$).

(ii) The second feature is the existence of wakes. Two types of wake can be distinguished: on the hub side ($z/b < 0.5$), the wakes of the trailing edges of both the splitter and the full blades appear as sharp narrow areas of low flow angle. These are the genuine blade wakes. On the shroud side ($z/b > 0.5$), the wake is broadened due to the channel wake originating from the jet/wake type flow patterns that are typical for centrifugal impeller flow (e.g. Eckardt 1975, Dean and Senoo 1960). The channel
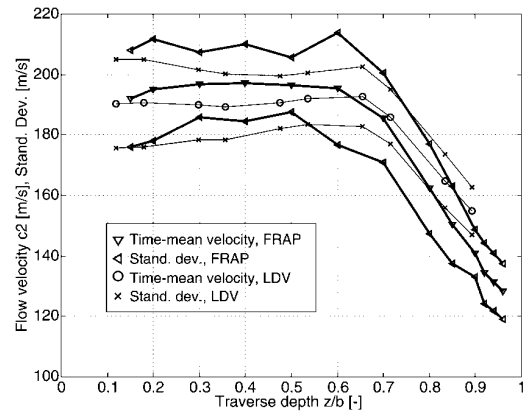

Figure 30. Time-mean absolute mean velocity and standard superposed deviation of the FRAP and LDV measurements. Note the stretched velocity scale.

wake of the suction side of the splitter blade is sharper than the channel wake following the full blade.

The comparison of the two measurement techniques shows that both systems equally capture these main flow features. Even the difference of the channel wake width downstream of full and splitter blades is equally visible. Furthermore a good agreement of the two measurement techniques in terms of the flow angle level can be seen.

Another comparison was made by calculating the time-mean values (and the standard deviations) for each traverse position for both systems.

In figure 30 the time-mean absolute velocity at the impeller exit is plotted over the channel depth. Both the absolute level and its variation over the traverse depth correspond quite well remembering that the physical bases of the two methods are totally different.

6.4. Rotating stall in a centrifugal compressor

By applying suitable measurement and data evaluation concepts the systematic flow structures of rotating stall (RS) can be measured and evaluated with a one-sensor probe. This procedure is described in detail in Roduner *et al* (1999b) and Roduner (1999).

For these measurements the test rig was operated at Mu = 0.4, where RS could be maintained as a stable phenomenon. For the present stage configuration single-cell full span rotating stall was observed.

Class-averaged data are presented in figure 31 and 32. In figure 31 the radial velocity (c_r) is plotted from hub to shroud in order to show that during RS the entire channel is temporarily blocked. One can easily distinguish between sound flow areas and areas where reverse flow passes the probe ($0.4 < t/\Delta t_{RS} < 0.65$).

Figure 32 shows the mid-channel radial velocity component as well as the static and total pressure variation for one RS period. Seen from the absolute (non-rotating) frame of the probe located at Position I ($r^* = 1.05$), the following phenomena during one RS period starting at $t/\Delta t_{RS} = 0$ can be observed. The passage of one RS period, i.e., one circumferential rotation of a RS cell, can be divided into four sections.
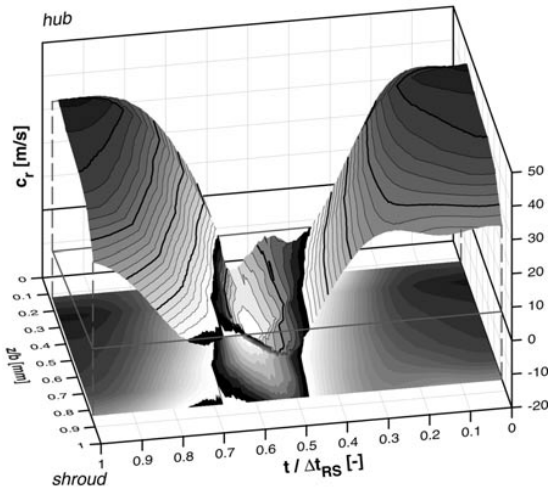
Figure 31. Class-averaged radial velocity measured at the impeller exit over one rotating stall period.
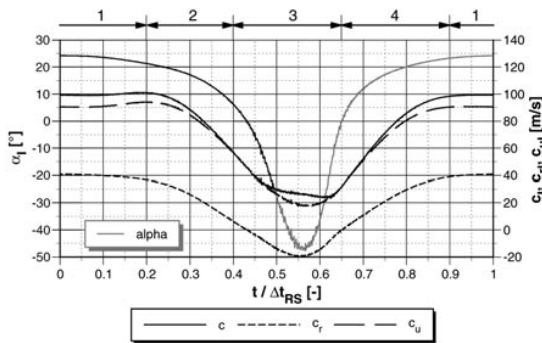

Figure 32. Class-averaged radial velocity, static and total pressure distribution, measured at the impeller exit ($z/b = 0.48$).

(i) ($t/\Delta t_{RS} = 0.9$–0.2). The sound flow of non-blocked impeller channels with positive c_r values passes the probe.

(ii) ($t/\Delta t_{RS} = 0.2$–0.4). The velocity drops and the flow angle α_2 decreases. Total and static pressure decrease and approach each other.

(iii) ($t/\Delta t_{RS} = 0.4$–0.65). Now the probe is downstream of the blocked impeller channels. c_r is low and negative. Dynamic head is small due to the small velocities. The static pressure is increasing.

(iv) ($t/\Delta t_{RS} = 0.65$–0.9). The stagnant fluid is blown away by sound throughflow coming from the impeller. Velocity and α increase. Due to the acceleration of the flow the static pressure decreases.

In Gyarmathy (1996) RS is described as impeller–diffuser momentum exchange. This model is in good agreement with the measured pressure traces during one RS period. Stopping and reversing the forward flow is associated with a static pressure minimum in the impeller/diffuser interspace, while its re-start requires a pressure maximum. The edges of the cell ($c_r = 0$) closely coincide with the static pressure peaks. The pressure amplitudes downstream of the diffuser (not shown) are small.

7. Conclusions

Fast-response probes provide the local time history of total and static pressure, flow angles and velocity of highly fluctuating flows. Some of these flow quantities cannot be provided by other measuring techniques. Therefore the different fast-response measurement techniques can be considered as complementary to each other, but not competitive.

In the last decades the fast-response probe measurement technique has gone through a thorough development process of its main components to reach the present state. The keys for accurate DC and AC measurements are the choice of appropriate and small sensors combined with a probe tip, which exhibits good aerodynamic characteristics in highly fluctuating flows and a high-quality calibration of both the sensor and probe characteristics.

To avoid systematic sensor errors the micro fabrication, the chip technology and the packaging technique have to be optimized in order to assure a reliable sensor signal and to achieve the smallest probe tip possible. Probe designs with the active side of the sensor membrane turned towards the probe interior restrict the frequency response typically to 80–90 kHz, but provide a robust probe with a high geometric precision of the tip.

A careful calibration of the sensors and a comprehensive aerodynamic calibration of the probe are important points for the accurate measurement of the time-varying quantities. The calibration of the pressure sensors concerning the static and dynamic properties provide a reliable measurement of the sensor pressure values at large flow angle variations. For this reason a large angular calibration range of the probe is required. The dynamic (transient) aerodynamic behaviour is another important issue. Circular-cylinder shapes combine good dynamic characteristics with a large angular calibration range suitable for data evaluation.

Auxiliary parts of the measurement system such as the pneumatic support and control module of the probe, the traverse system, the control computer with the graphical user interface, the monitoring system and the data acquisition system with analogue filters and A/D converters have to be improved continuously to enhance the accuracy.

The data processing contains the data conversion from voltages into flow quantities and the data analysis where phase-averaging and other physically meaningful averaging methods are applied. The existing frequencies are analysed or separated and statistical methods are used. All these topics of the data processing should be included in user friendly software to extract the interesting information from the huge amount of time-resolved data.

Turbomachinery flows being highly three-dimensional, multi-sensor probes (with at least four sensors to give three velocity components) are of great interest, with three sensors being acceptable in predominantly two-dimensional flow fields. Such multi-sensor probes have been developed by various research groups using different geometric shapes.

Much experience has been collected by the authors' group with straight cylindrical probes and with the measurement system needed to operate fast-response probes. An interesting result of these investigations was to realize

that the relatively simple and thin single-sensor probes can provide quite complete flow information. The application of the probe system in centrifugal compressor flow showed the robustness of the probe design in real rough turbomachine flows and the accuracy of the results obtained. Comparisons with pneumatic probe measurements for the DC information and LDV comparisons for the time-resolved measurements were successful, proving the maturity of fast-response probe systems.

References

Adamczyk J J 1986 *A Model for Closing the Inviscid Form of the Average-Passage Equation System* ASME 86-GT-227

Ainsworth R W, Allen J L and Batt J J M 1995 The development of fast response aerodynamic probes for flow measurements in turbomachinery *ASME J. Turbomachinery* **117** 625–34

Ainsworth R W, Dietz A J and Nunn T A 1990 The use of semi-conductor sensors for blade surface pressure measurement in a model turbine stage *ASME Gas Turbine and Aeroengine Congress (Rhode-Saint-Genèse)* 90-GT-346

Arts T, Dénos R, Brouckaert J-F and Popp O 1996 The dual hot wire aspirating probe *Proc. 13th Symp. on Measuring Techniques for Transonic and Supersonic Flows in Cascades and Turbomachines (Zurich)*

Belhabib M and Miton H 1995 Experimental analysis of unsteady blade rows interaction in a multistage turbomachine *J. Physique* III

Bendat J and Piersol A 1991 *Engineering Applications of Correlation and Spectral Analysis* (New York: Wiley)

Bergh H and Tijdeman H 1965 Theoretical and experimental results for the dynamic response of pressure measuring systems *NLR–TRF* p 283

Binder J 1989 Piezoresistive Silizium-Drucksensoren *Halbleiter-Sensoren* (Ehningen: Expert) ed H Reichl

Binder A, Schroeder Th and Hourmouziadis J 1989 Turbulence measurements in a multistage low-pressure turbine *J. Turbomachinery* April

Bohn D and Simon H 1975 Mehrparametrige Approximation der Eichräume und Eichflächen von Unterschall- bzw. Überschall-5-Loch-Sonden *ATM Messtechnische Praxis* p 470

Brouckaert J F, Sieverding C H and Manna M 1998 Development of a fast response 3-hole pressure probe *Proc. 14th Symp. on Measuring Techniques in Transonic and Supersonic Flows in Cascades and Turbomachines (Limerick)*

Bryer D W and Pankhurst R C 1971 *Pressure-Probe Methods for Determining Wind Speed and Flow Direction* (London: Her Majesty's Stationery Office)

Bubeck H and Wachter J 1987 Development and application of a high frequency wedge probe *ASME Paper* 87-GT-216

Capece V R and Fleeter S 1989 Measurement and analysis of unsteady flow structures in rotor blade wakes *Experiment in Fluids* (Berlin: Springer)

Cherrett M A 1990 Temperature error compensation applied to pressure measurements taken with miniature semiconductor pressure transducers in a high-speed research research compressor *Proc. 10th Symp. on Measuring Techniques in Transonic and Supersonic Flows in Cacades and Turbomachines (Rhode-Saint-Genèse)*

Cherrett M A, Bryce J D and Ginder R B 1995 Unsteady three-dimensional flow in a single-stage transonic fan: Part I—Unsteady rotor exit flow field *J. Turbomachinery* **117** 506–13

Chue S H 1975 Pressure probes for fluid measurement *Prog. Aerospace Sci.* **16** 147–223

Cook S C P 1989 Development of a high response aerodynamic wedge probe and use in a high speed research compressor *Proc. 9th Int. Symp. on Air Breathing Engines (Athens)* ISABE 89-7118

Dambach R and Hodson HP 1999 A new method of data reduction for single-sensor pressure probes *ASME 99-GT-304*

Dean R C Jr and Senoo Y 1960 Rotating wakes in vaneless diffusers *J. Basic Eng.* **82** 563–74

Dzung L 1967 Mittelungsverfahren in der Theorie der Schaufelgitter *Mitteilungen v. Brown Boveri*

Eckardt D 1975 Measurements in the jet-wake discharge flow of a centrifugal compressor impeller *J. Eng. Power* **97** 337–46

Epstein A H 1985 High frequency response measurements in turbomachinery *Measurement Techniques in Turbomachines (VKI Lecture Series 1985-03) (Rhode-Saint-Genèse)*

Evans R L 1975 Turbulence and unsteadiness measurements downstream of a moving blade row *J. Eng. Power* January

Gizzi W P 2000 Dynamische Korrekturen für schnelle Strömungssonden in hochfrequent fluktuierenden Strömungen [Dynamic corrections for fast-response probes in highly fluctuating flows] *PhD Thesis* No 13482 ETH Zurich

Gizzi W P and Gyarmathy G 1998 Correction procedures for fast-response probes *Proc. 14th Symp. on Measuring Techniques for Transonic and Supersonic Flows in Cascades and Turbomachines (Limerick)*

Gizzi W, Roduner C, Stahlecker D, Köppel P and Gyarmathy G 1999 Time-resolved measurements with fast-response probes and laser-Doppler-velocimetry at the impeller exit of a centrifugal compressor—a comparison of two measurement techniques *IMechE J. Power Energy* B **213** 291–308

Gossweiler C 1993 Sonden und Messsystem für schnelle aerodynamische Strömungsmessung mit piezoresistiven Druckgebern *PhD Thesis* ETH Zurich No 10253

——1996 Flow in radial turbomachines—unsteady measurements with fast-response probes *VKI Lecture Series 1996-01 (Rhode-Saint-Genèse)*

Gossweiler C, Humm H J and Kupferschmied P 1990 The use of piezoresistive semi-conductor pressure transducers for fast-response probe measurements in turbomachinery *Proc. 10th Symp. on Measuring Techniques for Transonic and Supersonic Flows in Cascades and Turbomachines (Rhode-Saint-Genèse)*

Gossweiler C, Kupferschmied P and Gyarmathy G 1995 On fast-response probes Part 1: Technology. Calibration and application to turbomachinery *J. Turbomachinery* **117** 611–17

Gostelow J 1977 A new approach to the experimental study of turbomachinery flow phenomena *J. Eng. Power* **99** 97–105

Gyarmathy G 1996 Impeller-diffuser momentum exchange during rotating stall *ASME Paper* 96-WA/PID-6

Heneka A 1983 Entwicklung und Erprobung einer Keilsonde für instationre dreidimensionale Strömungsmessungen in Turbomaschinen *Mitteilungen des Institutes* vol 14, Institut für Thermische Strömungsmaschinen und Maschinenlaboratorium der Universität Stuttgart

Humm H J 1996 Optimierung der Sondengestalt für aerodynamischen Messungen in hochgradig fluktuierenden strömungen [Probe-shape optimization for aerodynamic measurements in highly fluctuating flows] *PhD Thesis* ETH Zurich No 11661

Humm H J, Gizzi W P and Gyarmathy G 1994 Dynamic response of aerodynamic probes in fluctuating 3D flows *Proc. 12th Symp. on Measuring Techniques for Transonic and Supersonic Flows in Cascades and Turbomachines (Prague)*

Humm H J and Verdegaal J I 1992 Aerodynamic design criteria for fast-response probes *Proc. 11th Symp. on Measuring Techniques for Transonic and Supersonic Flows in Cascades and Turbomachines (Rhode-Saint-Genèse)*

Kerrebrock J L, Epstein A H, Haines D M and Thompkins W T 1974 The MIT Blowdown Compressor Facility *Trans. ASME* 74-GT-47

Kerrebrock J L, Thompkins W T and Epstein A H 1980 A miniature high frequency sphere probe *Measurement Methods in Rotating Components of Turbomachinery* ed B Lakshminarayana and P W Runstadtler (New York: ASME)

Köppel P 2000 Analyse von zeitabhängigen Messdaten aus Strömungssonden angewendet auf instationäre Turbomaschinenströmungen [Processing and application of time-resolved data measured with fast-response aerodynamic probes in turbomachinery flows] *PhD Thesis* ETH Zurich, at press

Köppel P, Roduner C, Kupferschmied P and Gyarmathy G 1999 On the development and application of the FRAP® (fast-response aerodynamic probe) system in turbomachines—Part 3: Comparison of averaging methods applied to centrifugal compressor measurement *ASME 99-GT-154*

Kovasznay L S G, Tani I, Kawamura M and Fujita H 1981 Instantaneous pressure distribution around a sphere in unsteady flow *J. Fluid Engng* **103** December

Krause L N and Dudzinski T J 1969 Flow direction measurement with fixed position probes in subsonic flows over a range of Reynolds numbers *NASA TMX-52576* May

Kreitmeier F 1987 A new time-averaging procedure for compressible unsteady turbulent flows *ASME 87-GT-83*

Kupferschmied P 1998 Zur Methodik zeitaufgelöster Messungen mit Strömungssonden in Verdichtern und Turbinen [On the methodology of time-resolved measurements with aerodynamic probes in compressors and turbines] *PhD Thesis* ETH Zurich No 12774

Kupferschmied P, Gossweiler C and Gyarmathy G 1994 Aerodynamic fast-response probe measurement systems: state of development, limitation and future trends *Proc. 12th Symp. on Measuring Techniques for Transonic and Supersonic Flows in Cascades and Turbomachines (Prague)*

Kupferschmied P, Köppel P, Roduner C and Gyarmathy G 1999 On the development and application of the FRAP® (fast-response aerodynamic probe) system for turbomachines—Part 1: The measurement system *ASME International Gas Turbine and Aeroengine Congr. (Indianapolis)* ASME 99-GT-152

Kupferschmied P, Roduner C and Gyarmathy G 1998 Some considerations on using miniature pressure sensors in fast-response aerodynamic probes for flow temperature measurements *Proc. 14th Symp. on Measuring Techniques in Transonic and Supersonic Flows in Cascades and Turbomachines (Limerick)*

Lakshminarayana B 1981 Techniques for aerodynamic and turbulence measurements in turbomachinery rotors *ASME J. Eng. Power* **103** 375–92

Larguier R 1985 Experimental analysis methods for unsteady flows in turbomachines *7th Int. Symp. on Air Breathing Engines (Beijing)*

Larguier R and Ruyer C 1972 Méthode d'analyse expérimentale de l'écoulement instationnaire dans un compresseur aéronautique transsonique *Recherche Aérospatiale* **6** 353–6

Lisec T, Kreutzer M and Wagner B 1996 Surface micromachined piezoresistive pressure sensors with step-type bent and flat membrane structures *IEEE Trans. Electron. Devices* **43** No 9

Matsunaga S, Ishibashi H and Nishi M 1978 Accurate measurement of non-steady three-dimensional incompressible flow by means of a combined five-hole probe *Nonsteady Fluid Dynamics, Winter ASME Meeting (San Francisco)*

Ng W F and Epstein A H 1983 High-frequency temperature and pressure probe for unsteady compressible flows *Rev. Sci. Instrum.* **54**

Ng W F and Epstein A H 1985 Unsteady losses in transonic compressors *J. Eng. Gas Turbines Power* **107** 345–53

Ng W F and Popernack T G 1987 A combination probe for high-frequency unsteady aerodynamic measurements in transonic wind tunnels *Int. Congr. on Instrumentation in Aerospace Simulation Facilities (Williamsburg, VA)*

Rieß W and Walbaum M 1994 Meßtechnische Erfassung instationärer Strömungsvorgänge in mehrstufigen Axialverdichtern *Mitt. Pfleiderer-Institut für Strömungsmaschinen* vol 1 (Braunschweig: Faragallah)

Roduner C 1999c Strömungsstrukturen in Radialmaschinen, untersucht mit schnellen Sonden [Flow structures in centrifugal compressors measured with fast-response aerodynamic probes] *PhD Thesis* No 13428 ETH Zurich

Roduner C, Köppel P, Kupferschmied P and Gyarmathy G 1999a Comparison of measured integral averages at the impeller exit of a centrifugal compressor measured with both pneumatic and fast-response probes *ASME J. Turbomachinery* **121** 609–18

Roduner C, Kupferschmied P, Köppel P and Gyarmathy G 1999b On the development and application of the FRAP (fast-response aerodynamic probe) system for turbomachines—Part 2: Flow, surge and stall in a centrifugal compressor *ASME Paper* 99-GT-153

Senoo Y, Kita Y and Ookuma K 1973 Measurement of two dimensional periodic flow with a cobra probe *ASME J. Fluids Eng.* June

Sentker A and Riess 1996 Turbulence intensity measurements in a low speed axial compressor *3rd Int. Symp. on Engineering Turbulence Modelling and Measurements (Crete)*

Shreeve R and Neuhoff F 1984 Measurements of the flow from a speed compressor rotor using a dual probe digital sampling (DPDS) technique *ASME J. Eng. Gas Turbines and Power*

Shreeve R, Simmons J, West J and Winters K 1978 Determination of transonic compressor flow field by synchronized sampling of stationary fast response transducers *ASME J. Eng. Gas Turbines and Power*

Sieverding C H, Arts T, Dénos R and Brouckaert J F 2000 Measurement techniques for unsteady flows in turbomachines *Exp. Fluids* **28** No 4

Stahlecker D and Gyarmathy G 1998 Investigations of turbulent flow in a centrifugal compressor vaned diffusor by 3-component laser velocimetry *ASME Paper* 98-GT-300

Traupel W 1982 *Thermische Turbomaschinen* Parts I and II (Berlin: Springer)

Treaster A L and Yocum A M 1979 The calibration and application of five-hole probes *ISA Trans.* **18** No 3